

Phase transition of interacting Bose gases in general power-law potentials

O. Zobay, G. Metikas, and G. Alber

Institut für Angewandte Physik, Technische Universität Darmstadt, 64289 Darmstadt, Germany

(Received 6 February 2004; published 23 June 2004)

We investigate the phase transition of interacting Bose gases in general power-law traps in the thermodynamic limit. Using energy-shell renormalization and the ε expansion, we evaluate the partition function for the uncondensed gas phase within a renormalization-group framework. This approach allows a unified description of homogeneous as well as inhomogeneous and anisotropic systems. Results for the critical temperature are compared to mean-field theory as well as to a local-density approximation based on renormalization-group theory for the homogeneous Bose gas. This comparison indicates the consistency of our approach. We also make suggestions for an optimized trap design in experiments that measure the transition temperature.

DOI: 10.1103/PhysRevA.69.063615

PACS number(s): 03.75.Hh, 05.30.Jp, 64.60.Ak

I. INTRODUCTION

The recent realization of Bose-Einstein condensation (BEC) in dilute atomic vapors [1–3] has renewed interest in the quantum-statistical properties of weakly interacting Bose gases around the phase transition. So far, research in this area has mainly focused on the spatially uniform system and, as a key question, the dependence of its condensation temperature T_c on the atomic interactions [4]. The particular theoretical challenge of this system is rooted in the fact that near the transition point its behavior is dominated by long-wavelength critical fluctuations that cannot be treated perturbatively. Because of these difficulties, a generally accepted result for the condensation temperature has emerged only very recently [5,6] and after a long and controversial debate.

Compared to the homogeneous case, the study of condensation in trapped Bose systems, although of immediate experimental relevance, has received considerably less attention. Presumably, this is due to the fact that to leading order in the atomic interaction, the shift in T_c is determined by mean-field effects. The shift was first calculated in Ref. [7], and the result found there has subsequently been verified by a number of different numerical approaches [8–11] (although this result is now generally accepted [12–15], there exist a few slightly [16–18] and strongly [19] deviating works in the literature). In spite of the unanimity regarding the leading-order behavior, the situation for larger interaction strengths, where effects beyond mean-field theory are expected to become significant, is much less clear. Most studies agree that, similar to the homogeneous case, critical fluctuations lead to an increase in T_c as compared to the mean-field result [10,11,13,15]. The quantitative extent of the increase, however, varies between the different works. On the other hand, Ref. [9], using a variational approach with a Morse interaction potential, finds an additional decrease in T_c .

Recently, precise experimental measurements of the shift in T_c as a function of the effective atomic interaction strength have become available [20], and the results can be considered well compatible with mean-field theory. Nevertheless, it is interesting to note that the measured value of the corresponding proportionality constant varies by more than 20% from the theoretical prediction, although this difference is still within the experimental error range. At any rate, the experiment has entered a regime for the interaction strength

where most theories predict observable, yet varying, deviations from the mean-field result [10,11,13,15]. In view of the experimental progress and continuing theoretical uncertainties, further investigations into the phase transition of trapped Bose gases are certainly well justified.

Renormalization-group (RG) methods provide one possible pathway for studying the critical behavior of Bose gases beyond mean-field theory. Following, in particular, the work of Refs. [21,22], we have recently formulated a RG treatment for harmonically trapped Bose gases [11] which is based on energy-shell renormalization and the ε expansion. The purpose of the present paper is to generalize our approach to a broader class of potentials and to apply it to the investigation of Bose condensation in generic power-law traps in the thermodynamic limit.

Our motivation for this study is twofold. First of all, although our results for harmonically trapped atoms [11] compare reasonably well with other approaches, it is necessary to test our RG method in a broader context in order to better establish its range of validity and to rule out a coincidental agreement. Often, and also in our case, renormalization-group calculations contain uncontrolled approximations, so that their results and predictions should always be checked carefully. For our purposes, the study of power-law traps is particularly appealing as they provide a natural interpolation between homogeneous and harmonic confinement. Furthermore, both ideal [23–28] and interacting [12,29–33] Bose gases in power-law traps have been studied before, and a number of useful analytical results are already available—e.g., for the density of states and the condensation temperature in the ideal case. In order to test our RG results for power-law traps, we compare them to mean-field theory as well as to a local-density approximation based on the RG description of the uniform gas (RG-LDA). The comparison with the RG-LDA allows for a self-consistency check of our method.

Our second motivation is to obtain a more thorough physical understanding of the dependence of the BEC phase transition on the trapping potentials. In particular, we are interested in investigating the crossover between the homogeneous potential, where the condensation process is dominated by long-range critical fluctuations, and more inhomogeneous potentials, where mean-field potential shape effects are prevalent. Furthermore, we consider more practical is-

sues such as finding trap parameters that maximize the shift in the critical temperature from the ideal to the interacting gas or determining the conditions under which effects beyond mean-field theory are most prominent. Our study also yields information about circumstances under which the dependence of T_c on the effective interacting strength is particularly sensitive or stable with respect to variations of the external potential. We thus expect that our results provide some insight that is useful for the development of traps specifically designed for observing condensation phenomena.

The article is organized as follows. In Sec. II, the physics of ideal Bose gases in power-law potentials is reviewed briefly. In Sec. III, we introduce the RG method and describe how to extend our treatment of interacting Bose gases in isotropic harmonic traps [11] to more general trapping potentials. Alternative approaches to BEC in external potentials, which are based on the local-density approximation, are presented in Sec. IV. We discuss mean-field theory and the approach based on the RG theory for the homogeneous gas. Section V is devoted to the comparison and discussion of results from our RG method, the RG-LDA, and mean-field theory. The presented material indicates that the renormalization group indeed provides a consistent description of the phase transition for the systems under consideration. Section VI contains a short summary.

II. IDEAL BOSE GASES IN POWER-LAW TRAPS

In this section we summarize some results about ideal Bose gases in power-law traps. The notation follows Refs. [12,23]. We consider a system of N ideal bosons of mass m which are trapped in a power-law potential

$$V(\mathbf{r}) = E_1 \left| \frac{x}{L_1} \right|^p + E_2 \left| \frac{y}{L_2} \right|^l + E_3 \left| \frac{z}{L_3} \right|^s. \quad (1)$$

We introduce the constant

$$\eta = \frac{1}{p} + \frac{1}{l} + \frac{1}{s} + \frac{1}{2}, \quad (2)$$

which characterizes the potential shape, and the characteristic volume

$$V_{\text{char}}^{2(\eta+1)/3} = 8 \left(\frac{\hbar^2}{m} \right)^{\eta-1/2} \frac{L_1 L_2 L_3 I(p, l, s)}{E_1^{1/p} E_2^{1/l} E_3^{1/s}}, \quad (3)$$

with $I(p, l, s) = \Gamma(1/p)\Gamma(1/l)\Gamma(1/s)/p l s$ and $\Gamma(x)$ the gamma function. Note that in the homogeneous case ($p=l=s=\infty$) $V_{\text{char}} = 8L_1 L_2 L_3$ and in the harmonic case ($p=l=s=2$) $V_{\text{char}} = (2\pi)^{3/4} a_{ho}^{(x)} a_{ho}^{(y)} a_{ho}^{(z)}$ with $a_{ho}^{(i)}$ the usual harmonic oscillator length.

In the semiclassical approximation, the number of single-particle states up to the energy ε is obtained as [24]

$$\Sigma(\varepsilon) = \frac{1}{(2\pi\hbar)^3} \int_{H \leq \varepsilon} d^3 r d^3 p = \frac{V_{\text{char}}^{2(\eta+1)/3}}{(2\pi)^{3/2} \Gamma(\eta+2)} \left(\frac{m}{\hbar^2} \right)^{\eta+1} \varepsilon^{\eta+1}, \quad (4)$$

so that the density of states is given by

$$D(\varepsilon) = \frac{d\Sigma(\varepsilon)}{d\varepsilon} = \frac{V_{\text{char}}^{2(\eta+1)/3}}{(2\pi)^{3/2} \Gamma(\eta+1)} \left(\frac{m}{\hbar^2} \right)^{\eta+1} \varepsilon^{\eta}. \quad (5)$$

For calculations in the mean-field and local-density approximations, it is useful to convert certain spatial integrations according to $\int d^3 r f[V(\mathbf{r})] = \int d\varepsilon \tilde{\rho}(\varepsilon) f(\varepsilon)$. In this way, isotropic and anisotropic power-law potentials can be treated on the same footing. The density $\tilde{\rho}(\varepsilon)$ can be regarded as the ‘‘equipotential surface area’’ of $V(\mathbf{r})$ at energy ε . It is given by

$$\tilde{\rho}(\varepsilon) = \frac{V_{\text{char}}^{2(\eta+1)/3}}{\Gamma(\eta-1/2)} \left(\frac{m}{\hbar^2} \right)^{\eta-1/2} \varepsilon^{\eta-3/2}. \quad (6)$$

Note that in the homogeneous case $\tilde{\rho}(\varepsilon) = V_{\text{char}} \delta(\varepsilon)$. Equation (6) can be derived by considering the Hamiltonian

$$H(\mathbf{p}, \mathbf{r}) = \begin{cases} V(\mathbf{r}), & |\mathbf{p}| < p_0, \\ \infty, & |\mathbf{p}| \geq p_0, \end{cases}$$

with arbitrary $p_0 > 0$. For this Hamiltonian, the semiclassical number of states is given by [24]

$$\Sigma(\varepsilon) = \frac{1}{6\pi^2 \hbar^3} \frac{V_{\text{char}}^{2(\eta+1)/3}}{\Gamma(\eta+1/2)} p_0^3 \left(\frac{m}{\hbar^2} \right)^{\eta-1/2} \varepsilon^{\eta-1/2}.$$

On the other hand, we have $(2\pi\hbar)^3 \Sigma(\varepsilon) = \frac{4}{3} \pi p_0^3 \int_{V \leq \varepsilon} d^3 r = \frac{4}{3} \pi p_0^3 \int_0^\varepsilon d\varepsilon' \tilde{\rho}(\varepsilon')$, from which Eq. (6) follows.

In the following, we wish to focus on the thermodynamic limit, which is defined by $N V_{\text{char}}^{-2(\eta+1)/3} = \text{const}$, $N, V_{\text{char}} \rightarrow \infty$. The equation of state for the ideal Bose gas above the condensation point is then given by [24,26]

$$N = \int_0^\infty d\varepsilon D(\varepsilon) \frac{1}{e^{\beta(\varepsilon-\mu)} - 1} = \frac{1}{(2\pi)^{3/2}} \left(\frac{m}{\hbar^2 \beta} \right)^{\eta+1} V_{\text{char}}^{2(\eta+1)/3} g_{\eta+1}(z), \quad (7)$$

with β the inverse temperature, μ the chemical potential, and $z = \exp(\beta\mu)$ the fugacity. The Bose functions are defined by $g_\lambda(z) = \sum_{k=1}^\infty z^k / k^\lambda$. The spatial density distribution of the gas is determined by the relation

$$n(\mathbf{r}) = \lambda_T^{-3} g_{3/2} \{ \exp[\beta(\mu - V(\mathbf{r}))] \}, \quad (8)$$

with the thermal wavelength $\lambda_T = (2\pi\hbar^2 \beta / m)^{1/2}$. The condition for Bose-Einstein condensation, which follows from setting $z=1$ in Eq. (7) or evaluating $N = \int d^3 r n(\mathbf{r}, \mu=0)$ from Eq. (8), reads [23]

$$N = \frac{1}{(2\pi)^{3/2}} \left(\frac{m}{\hbar^2 \beta_c^0} \right)^{\eta+1} V_{\text{char}}^{2(\eta+1)/3} \zeta(\eta+1), \quad (9)$$

with $\beta_c^0 = 1/k_b T_c^0$ the inverse critical temperature and $\zeta(x)$ the Riemann ζ function.

III. RENORMALIZATION-GROUP DESCRIPTION OF TRAPPED BOSE GASES

In this section, we generalize our renormalization-group description of harmonically trapped Bose gases [11] to the

case of more general external potentials. Again, we work in the thermodynamic limit. We start from the functional integral representation of the grand-canonical partition function for the trapped interacting Bose gas, which is given by

$$Z = \int \delta[\phi, \phi^*] e^{-S[\phi, \phi^*]}. \quad (10)$$

We consider bosonic fields $\phi(\tau, \mathbf{x})$ and $\phi^*(\tau, \mathbf{x})$ that depend on D spatial coordinates $\mathbf{x}=(x_1, \dots, x_D)$ and on imaginary time τ . The fields are periodic in τ with period $\hbar\beta$, where $\beta=1/k_B T$ is the inverse temperature and k_B denotes Boltzmann's constant. The Euclidean action appearing in the functional integral of Eq. (10) is determined by

$$S[\phi, \phi^*] = \frac{1}{\hbar} \int_0^{\hbar\beta} d\tau \int d^D \mathbf{x} \left\{ \phi^*(\tau, \mathbf{x}) \left[\hbar \frac{\partial}{\partial \tau} - \frac{\hbar^2}{2m} \nabla^2 + V(\mathbf{x}) - \mu \right] \phi(\tau, \mathbf{x}) + \frac{g}{2} |\phi(\tau, \mathbf{x})|^4 \right\}. \quad (11)$$

The short-range repulsive interaction potential between the atoms is characterized by the coupling constant g . Its relation to the scattering length a is given below [Eq. (21)]. The external trapping potential $V(\mathbf{x})$ denotes the D -dimensional generalization of Eq. (1). As $V(\mathbf{x})$ is separable, we can define the sets of eigenfunctions $\psi_{n_j}^{(j)}(x_j)$, $j=1, \dots, D$, $n_j=1, \dots, \infty$, with eigenenergies $E_{n_j}^{(j)}$ for the D spatial dimensions.

We now expand the Bose fields appearing in Eq. (10) in terms of these eigenfunctions—i.e.,

$$\phi(\tau, \mathbf{x}) = \sum_{l=-\infty}^{\infty} \sum_{E(n_1, \dots, n_D) \leq E_\Lambda} \frac{e^{ip_0^l \tau}}{\sqrt{\hbar\beta}} \psi_{n_1}^{(1)}(x_1) \dots \psi_{n_D}^{(D)}(x_D) \times \tilde{\phi}(l, n_1, \dots, n_D),$$

with $p_0^l = 2\pi l / \hbar\beta$ the Matsubara frequencies and $\tilde{\phi}(l, n_1, \dots, n_D)$ complex-valued expansion coefficients. We also impose a high-energy cutoff condition on the expansion by only including those products $\psi_{n_1}^{(1)}(x_1) \dots \psi_{n_D}^{(D)}(x_D)$ of eigenfunctions whose total energy $E(n_1, \dots, n_D) = \sum_j E_{n_j}^{(j)}$ is less than the cutoff energy $E_\Lambda = \hbar^2 \Lambda^2 / 2m$.

To evaluate the partition function (10) above the phase transition, we apply a variant of the momentum-shell renormalization-group method [34] in which we successively integrate out thin energy shells starting at the cutoff energy E_Λ . To this end, the Bose fields are split into a high-energy and a low-energy part—i.e., $\phi(\tau, \mathbf{x}) = \phi_{<}(\tau, \mathbf{x}) + \phi_{>}(\tau, \mathbf{x})$, with

$$\phi_{>}(\tau, \mathbf{x}) = \sum_{l=-\infty}^{\infty} \sum_{E_\Lambda - \delta E_\Lambda \leq E(n_1, \dots, n_D) \leq E_\Lambda} \frac{e^{ip_0^l \tau}}{\sqrt{\hbar\beta}} \psi_{n_1}^{(1)}(x_1) \dots \psi_{n_D}^{(D)}(x_D) \times \tilde{\phi}(l, n_1, \dots, n_D).$$

The width δE_Λ of the high-energy shell is chosen to be small compared to the cutoff energy E_Λ . By integrating out the high-energy components of the Bose field in the partition function, we obtain an effective action for the low-energy

field $\phi_{<}$. The one-loop calculation of the effective theory yields [11,35,36]

$$S_{\text{eff}}(\phi_{<}, \phi_{<}^*) = S(\phi_{<}, \phi_{<}^*) + \frac{1}{2} \text{Tr} \{ \ln [(\hat{G}_0^>)^{-1} - \hat{\Sigma}] \}, \quad (12)$$

with $\hat{G}_0^>$ the bare Green's function for the high-energy field and $\hat{\Sigma}$ the self-energy for the low-energy field. The ‘‘Tr’’ symbol denotes the trace in both the functional and internal spaces of the operators. After expanding this trace up to second order in $\hat{G}_0^> \hat{\Sigma}$, the effective action reads

$$S_{\text{eff}}(\phi_{<}, \phi_{<}^*) \approx S(\phi_{<}, \phi_{<}^*) + \frac{1}{2} \text{Tr} [\ln (\hat{G}_0^>)^{-1}] - \frac{1}{2} \text{Tr} (\hat{G}_0^> \hat{\Sigma}) - \frac{1}{4} \text{Tr} [(\hat{G}_0^> \hat{\Sigma})^2]. \quad (13)$$

For the trace involving only $(\hat{G}_0^>)^{-1}$, the summation over the Matsubara frequencies yields the ideal-gas result

$$\frac{1}{2} \text{Tr} [\ln (\hat{G}_0^>)^{-1}] = - \sum_{E_\Lambda - \delta E_\Lambda \leq E(n_1, \dots, n_D) \leq E_\Lambda} \dots \sum \ln [1 - e^{-\beta(E_\Lambda - \mu)}], \quad (14)$$

whereas for the other traces we obtain

$$\text{Tr} [\hat{G}_0^> \hat{\Sigma}] = 4g N_{BE}(E_\Lambda) \times \int_0^{\hbar\beta} d\tau \int d^D \mathbf{x} |\phi_{<}(\tau, \mathbf{x})|^2 A(E_\Lambda, \delta E_\Lambda, \mathbf{x}) \quad (15)$$

and

$$\text{Tr} [\hat{G}_0^> \hat{\Sigma} \hat{G}_0^> \hat{\Sigma}] = 2g^2 \left\{ 4\beta N_{BE}(E_\Lambda) [1 + N_{BE}(E_\Lambda)] + \frac{1 + 2N_{BE}(E_\Lambda)}{2(E_\Lambda - \mu)} \right\} \int_0^{\hbar\beta} d\tau \int d^D \mathbf{x} |\phi_{<}(\tau, \mathbf{x})|^4 A(E_\Lambda, \delta E_\Lambda, \mathbf{x}), \quad (16)$$

with $N_{BE}(E) = [e^{\beta(E-\mu)} - 1]^{-1}$ the Bose-Einstein distribution. The function

$$A(E_\Lambda, \delta E_\Lambda, \mathbf{x}) = \sum_{E_\Lambda - \delta E_\Lambda \leq E(n_1, \dots, n_D) \leq E_\Lambda} \dots \sum |\psi_{n_1}^{(1)}(x_1) \dots \psi_{n_D}^{(D)}(x_D)|^2 \quad (17)$$

contains a summation over the squared moduli of all wave functions within the energy shell at point \mathbf{x} . In Ref. [11], $A(E_\Lambda, \delta E_\Lambda, \mathbf{x})$ was evaluated for the isotropic harmonic oscillator. However, the approach can be generalized to the much broader class of external potentials (1) if one focuses on the thermodynamic (or continuum) limit. In this case, the sum of Eq. (17) is dominated by highly excited wave functions which we can approximate by the WKB expression [37]

$$\begin{aligned} \psi_n^{(j)}(x) = & \sqrt{\frac{dE_n^{(j)}/dn}{\hbar \pi}} \frac{(2m)^{1/4}}{[E_n^{(j)} - V^{(j)}(x)]^{1/4}} \\ & \times \cos \left[\frac{1}{\hbar} \int_{a_n^{(j)}}^x dy \left(\sqrt{2m[E_n^{(j)} - V^{(j)}(y)]} - \frac{\pi}{4} \right) \right], \end{aligned} \quad (18)$$

with $V^{(j)}(x)$ the one-dimensional potential in the direction j , and $a_n^{(j)}$ and $b_n^{(j)}$ the left and right classical turning points defined by $E_n^{(j)} = V^{(j)}(a_n^{(j)}) = V^{(j)}(b_n^{(j)})$. Expression (18) is valid in the classically allowed region $a_n^{(j)} \leq x \leq b_n^{(j)}$ except for a small region near the turning points.

The thermodynamic limit is characterized by the fact that the length scales, over which the trapping potential changes, tend to infinity. On the other hand, typical energies, which are relevant for the RG calculations — such as the temperatures of interest or the chemical potential — and which determine the choice of the energy cutoff, remain constant. To a first degree of approximation, we can therefore shift the turning points appearing in the WKB expression (18) to infinity and also neglect the trapping potential $V^{(j)}(x)$ in the denominator. Furthermore, we make use of the fact that the energy shell of width δE_Λ contains a large number of eigenfunctions, so that the \cos^2 contributions appearing in Eq. (17) can safely be replaced by the averaged value of $1/2$.

Within these approximations we obtain $A(E_\Lambda, \delta E_\Lambda, \mathbf{x}) = (\partial/\partial E)Q(E, \mathbf{x})|_{E_\Lambda} \delta E_\Lambda$, where

$$\begin{aligned} Q(E, \mathbf{x}) = & \sum_{E(n_1, \dots, n_D) \leq E} \cdots \sum |\psi_{n_1}^{(1)}(x_1) \cdots \psi_{n_D}^{(D)}(x_D)|^2 \\ \simeq & \sum_{E(n_1, \dots, n_D) \leq E} \cdots \sum \frac{(2m)^{D/2}}{(2\pi\hbar)^D} \prod_{j=1}^D \frac{dE_{n_j}^{(j)}/dn_j}{\sqrt{E_{n_j}^{(j)}}} \\ = & \frac{(2m)^{D/2}}{(2\pi\hbar)^D} \frac{\Omega_D}{D} E^{D/2}, \end{aligned} \quad (19)$$

with $\Omega_D = 2\pi^{D/2}/\Gamma(D/2)$ the surface of a D -dimensional unit sphere. Thus, the function $A(E_\Lambda, \delta E_\Lambda, \mathbf{x})$ does not depend on \mathbf{x} anymore. The traces (15) and (16) can therefore be interpreted as giving rise to small corrections to the chemical potential μ and the coupling constant g in the effective action S_{eff} . The trace (14), on the other hand, yields the actual contribution to the partition function. We can now perform the Kadanoff transformation in which the effective action is cast into the form of the original action and the original cutoff is restored through a scaling transformation. This procedure leads to RG flow equations for μ and g , since these quantities are readjusted after each integration over an energy shell. All these steps are explained in detail in Ref. [11]. The flow equations finally read

$$\frac{dM(l)}{dl} = 2M(l) - 2\tilde{G}(l) \frac{\Omega_D}{(2\pi)^D} b(l)N(l),$$

$$\begin{aligned} \frac{d\tilde{G}(l)}{dl} = & (4-D)\tilde{G}(l) - \tilde{G}(l)^2 \frac{\Omega_D}{(2\pi)^D} b(l) \\ & \times \left\{ 4b(l)N(l)[1+N(l)] + \frac{1+2N(l)}{2[E_- - M(l)]} \right\}. \end{aligned} \quad (20)$$

Here, we have introduced the scaled quantities $M(l) = \beta_\Lambda \mu(l)$, $\tilde{G}(l) = \beta_\Lambda \Lambda^D g(l)/b(l)$, $b(l) = \beta e^{-2l}/\beta_\Lambda$, and $E_- = \beta_\Lambda E_\Lambda = 1/2$ with $\beta_\Lambda = m/\hbar^2 \Lambda^2$ the cutoff temperature. The function $N(l) = \{e^{b(l)[E_- - M(l)]} - 1\}^{-1}$ is the scaled Bose-Einstein distribution. The RG flow parameter l runs from 0 to ∞ as the physical cutoff is lowered according to Λe^{-l} in the course of integrating out the energy shells. The above l -dependent functions describe how the corresponding quantities change during the renormalization process. The initial conditions $M(0)$ and $b(0)$ are determined from the values of μ and β for the system of interest. The value of $\tilde{G}(0)$ is related to the s -wave scattering length of the atomic system according to [21,11]

$$a\Lambda = \frac{\tilde{G}(0)b(0)}{4\pi + \frac{2}{\pi}\tilde{G}(0)b(0)}. \quad (21)$$

The cutoff energy E_Λ should be chosen as the largest energy scale of the system so that typically $b(0), \tilde{G}(0) \gg 1$ and $M(0) \ll 1$. Note that Eqs. (20) only apply above the BEC phase transition— i.e., for a noncondensed gas.

In previous work, we have investigated the use of the ε expansion for the description of the BEC phase transition. First of all, it was shown that the ε expansion allows us to reconcile the differences between the flow equations derived for the homogeneous Bose gas in the symmetric and the symmetry-broken phase, respectively [38]. Furthermore, as discussed in [11], the ε expansion yields an improved result for the critical temperature T_c of the homogeneous gas at small scattering lengths, as well as a more plausible description of the behavior of T_c at large scattering lengths in harmonically trapped gases. Technically, the ε expansion amounts to expanding Eqs. (20) up to second order in $M(l)$ and $\tilde{G}(l)$. The flow equations then take the form

$$\begin{aligned} \frac{dM(l)}{dl} = & 2M(l) - 2\tilde{G}(l) \frac{\Omega_D}{(2\pi)^D} b(l) \{N_m(b(l)E_>) \\ & + b(l)N_m(b(l)E_>)[1+N_m(b(l)E_>)]M(l)\}, \\ \frac{d\tilde{G}(l)}{dl} = & \varepsilon\tilde{G}(l) - \tilde{G}(l)^2 \frac{\Omega_D}{(2\pi)^D} b(l) \left\{ \frac{1+2N_m(b(l)E_>)}{2E_>} \right. \\ & \left. + 4b(l)N_m(b(l)E_>)[1+N_m(b(l)E_>)] \right\}, \end{aligned} \quad (22)$$

with $N_m(x) = [\exp(x) - 1]^{-1}$ a modified Bose distribution. In $D=3$ dimensions, the flow equations (22) have to be integrated with $\varepsilon=4-D=1$. The ε expansion is expected to be applicable in the vicinity of the phase transition.

The flow equations (20) and (22), respectively, do not depend on the external trapping potential (1), and they also coincide with the RG equations for the homogeneous gas with periodic boundary conditions [21,22]. In other words, in our scheme the renormalization of μ and g becomes independent of the trapping potential in the thermodynamic limit. This is a consequence of the approximations leading to Eq. (19) in which we focus on the “bulk properties” of the system and neglect all surface effects.

The properties of the trap do come into play, however, when we calculate the free energy W of the system, from which, e.g., the critical temperature can be derived. Using Eqs. (5) and (14), one obtains

$$\begin{aligned} W &= -(\beta_\Lambda/\beta)\ln Z \\ &= \frac{\Lambda^{2(\eta+1)}V_{\text{char}}^{2(\eta+1)/3}}{(2\pi)^{3/2}\Gamma(\eta+1)2^\eta b(0)} \int_0^\infty dl e^{-2(\eta+1)l} \ln\{1 \\ &\quad - e^{-b(l)[1/2-M(l)]}\} \\ &\equiv \frac{\Lambda^{2(\eta+1)}V_{\text{char}}^{2(\eta+1)/3}}{(2\pi)^{3/2}\Gamma(\eta+1)2^\eta} I(M(0), \tilde{G}(0), b(0); \eta). \end{aligned} \quad (23)$$

The expression for W is identical to the ideal-gas case except that the chemical potential $M(l)$ is determined by the flow equations (20) or (22). The atomic interactions thus enter the calculation of W only through the renormalized chemical potential. The trapping potential essentially enters through its corresponding density of states which gives rise to the exponential factor $e^{-2(\eta+1)l}$. The term $I(M(0), \tilde{G}(0), b(0); \eta)$ appearing in Eq. (23) contains the integral from the preceding expression divided by $b(0)$; the notation is such that the dependence on the initial conditions for the flow equations becomes apparent.

The flow equations (20) or (22) can be used to describe the BEC phase transition as they possess a hyperbolic fixed point in the limit $l \rightarrow \infty$ which, for $D=3$, is located at $(M, \tilde{G}) = (1/12, 5\pi^2/72)$ or $(M, \tilde{G}) = (1/10, \pi^2/10)$, respectively. The flow trajectories asymptotically approaching the fixed point form the critical manifold; each of these critical trajectories describes a system at the phase transition with specific values of $M^{(cr)}(0)$, $\tilde{G}^{(cr)}(0)$, and $b^{(cr)}(0)$. The transition temperature T_c pertaining to a critical trajectory can be related to the particle number via the thermodynamic relation $N = -\partial W / \partial M(0)$. In this way, the shift in T_c with respect to an ideal gas with the same particle number (and the same trapping potential) is found as

$$\begin{aligned} &\left(\frac{T_c^{(RG)}}{T_c^{(0)}}\right)^{\eta+1} \\ &= -\frac{1}{b(0)^{\eta+1}} \frac{2^\eta \Gamma(\eta+1) \zeta(\eta+1)}{\frac{\partial}{\partial M(0)} I(M^{(cr)}(0), \tilde{G}^{(cr)}(0), b^{(cr)}(0); \eta)}. \end{aligned} \quad (24)$$

The scaled scattering length pertaining to the trajectory is given by

$$\frac{a}{\lambda_T^{(0)}} = \frac{\tilde{G}^{(cr)}(0)b^{(cr)}(0)}{4\pi + \frac{2}{\pi}\tilde{G}^{(cr)}(0)b^{(cr)}(0)} \frac{1}{\sqrt{2\pi b^{(cr)}(0)}} \left(\frac{T_c^{(0)}}{T_c^{(RG)}}\right)^{1/2}, \quad (25)$$

with $\lambda_T^{(0)}$ the thermal wavelength for the ideal gas at criticality. A discussion regarding the numerical aspects of evaluating Eqs. (24) and (25) can be found in [11].

The RG approach presented above relies on a number of essential approximations, regarding, for example, the derivative expansion, the polynomial expansion of the effective action in powers of the Bose fields, and the calculation of the function $A(E_\Lambda, \delta E_\Lambda, \mathbf{x})$ of Eq. (17) (for a more detailed discussion see, e.g., Refs. [11,36]). Some of the approximations involved are not completely systematic and controllable. One of the main purposes of this paper is to show that in spite of this unclarity the RG method provides a reliable and adequate tool to study the phase transition of Bose gases. To this end, it is important to compare results of RG calculations with other methods.

IV. LOCAL-DENSITY APPROXIMATIONS

An alternative approach to calculating the transition temperature of the trapped Bose gas is based on the local-density approximation (LDA). In the thermodynamic limit, the characteristic length scales of the trap (1) tend to infinity, so that the potential becomes locally flat at each point. Therefore, the trapped gas can locally be considered homogeneous with a chemical potential of $\mu - V(\mathbf{x})$, where μ denotes the global chemical potential of the gas. As a consequence, the spatial density n_{tr} of the trapped gas is related to the homogeneous density via

$$n_{tr}(\mathbf{x}) = n_{hom}(T, \mu - V(\mathbf{x})). \quad (26)$$

The BEC phase transition sets in at the trap center when the local chemical potential (which there equals the global chemical potential μ) reaches the critical value $\mu_c(T)$ of the homogeneous gas. We note that n_{tr} depends on position only through the potential $V(\mathbf{x})$. Thus we can invoke Eq. (6) together with Eq. (26) to examine the critical temperature T_c of an interacting Bose gas. From Eq. (9) follows that the change in T_c with respect to an ideal gas with the same particle number is given by

$$\left(\frac{T_c}{T_c^{(0)}}\right)^{\eta+1} = \frac{\zeta(\eta+1)\Gamma(\eta-1/2)}{\int dx x^{\eta-3/2} f_{cr}(x)}. \quad (27)$$

Here, $f_{cr}(x) = \lambda_T^3 n_{hom}(T_c, \mu_c(T_c) - x/\beta_c)$ denotes the dimensionless “degeneracy function” pertaining to the system at the phase transition. The variable $x = \beta_c V(\mathbf{x})$ measures the scaled distance in energy to the trap center. From Eq. (27) we see that the main influence of the trapping potential manifests itself in the weight factor $x^{\eta-3/2}$, with which the degeneracy function f_{cr} is multiplied under the integral and which originates from the density $\tilde{\rho}(\varepsilon)$ of Eq. (6). As expected, for η close to the value $1/2$ of the homogeneous system, the

relevant integration range is concentrated near $x=0$, whereas for growing η it is extended towards larger x .

The application of the LDA thus relies on an adequate determination of the degeneracy function $f_{cr}(x)$. In the following, we discuss two different approaches: mean-field theory (MFT), which has frequently been used before (e.g., [7,12,32]), and the renormalization group.

A. Mean-field theory

In MFT, the spatial density of an interacting homogeneous Bose gas above the condensation point is determined by the relation [39]

$$n_{hom}^{MF}(T, \mu) = \frac{1}{\lambda_T^3} g_{3/2} \{ \exp[\beta(\mu - 2U_0 n_{hom}^{MF})] \} \quad (28)$$

in the thermodynamic limit. Expression (28) is identical to the one for the ideal homogeneous gas [cf. Eq. (8)] except that the chemical potential is modified by the mean-field interaction potential $2U_0 n_{MF}(\mathbf{r})$ that is due to the atomic collisions. The coupling constant is given by $U_0 = 4\pi\hbar^2 a/m$ with a the s -wave scattering length. In the mean-field theory of interacting gases, BEC sets in when μ reaches its maximum value compatible with Eqs. (26) and (28). The critical chemical potential is thus determined by $\mu = 2U_0 n_{MF}(\mathbf{0})$. This implies a critical degeneracy of $n_{tr}^{MF}(\mathbf{0})\lambda_T^3 = \zeta(3/2)$ at the trap center just as for the ideal gas. Using these relations, the critical degeneracy function $f_{cr}^{MF}(x)$ can be obtained from Eq. (28) by solving the implicit equation

$$f_{cr}^{MF}(x) \equiv y = F_{3/2}(x - 4q[\zeta(3/2) - y]). \quad (29)$$

Here, $F_\lambda(x) = g_\lambda[\exp(-x)]$ denotes the Bose function and $q = a/\lambda_T$ the scaled interaction parameter.

For the homogeneous interacting Bose gas, mean-field theory yields the condensation condition $n_{hom}^{MF}\lambda_T^3 = \zeta(3/2)$. The condensation temperature $T_c^{(MF)}$ is thus not shifted in comparison to the noninteracting case. The actual shift of T_c is completely due to nonperturbative long-wavelength fluctuations of the Bose fields. For the harmonically trapped gas, however, the trapping potential effectively reduces the influence of the critical fluctuations [15]. The shift in the critical temperature is mainly determined by noncritical changes in the overall atomic density distribution that are caused by the atomic interactions. Mean-field theory is able to calculate this shift correctly to leading order in the atomic interactions [7].

For sufficiently inhomogeneous traps, mean-field theory thus yields quantitatively accurate results. For general power-law potentials, even in the quasihomogeneous limit $\eta \rightarrow 0.5$, MFT is useful as it provides at least a first approximation against which we can compare our other results. The mean-field theory of condensation in power-law potentials has been studied by several authors before [12,23,32,33]. However, these papers do not provide a complete coverage of the problem (in particular, the quasihomogeneous regime is not discussed properly), which gives an additional incentive to reconsider this question.

In general, the mean-field critical temperature for given set of system parameters η and q has to be determined numerically by solving Eq. (29) for $f_{cr}^{MF}(x)$ and performing the integration in Eq. (27). For small $q = a/\lambda_T$, however, the relative change $t_{MF} = 1 - T_c^{(MF)}/T_c^{(0)}$ in the critical temperature can be approximated as

$$t_{MF} = D_1(\eta)q + D'(\eta)q^{2\eta} + D_2(\eta)q^2 + o(q^2), \quad (30)$$

with

$$D_1(\eta) = -4c(\eta) \int_0^\infty dx x^{\eta-3/2} F_{1/2}(x) [\zeta(3/2) - F_{3/2}(x)], \quad (31)$$

$$D'(\eta) = -c(\eta)(16\pi)^\eta \frac{\Gamma(\eta+1/2)\Gamma(-\eta)}{\eta-1/2}, \quad (32)$$

$$D_2(\eta) = \frac{\eta+2}{2} D_1^2(\eta) - c(\eta) \int_0^\infty dx x^{\eta-3/2} \{ 8F_{-1/2}(x) [\zeta(3/2) - F_{3/2}(x)]^2 - 16F_{1/2}^2(x) [\zeta(3/2) - F_{3/2}(x)] \}, \quad (33)$$

and $c(\eta) = [(\eta+1)\Gamma(\eta-1/2)\zeta(\eta+1)]^{-1}$. This result, which is discussed in more detail in Ref. [40], has been derived from an expansion of the integral appearing in Eq. (27) in terms of q . It provides an accurate approximation of t_{MF} for all η and $q \lesssim 0.01$. In this way it extends the previous work of Refs. [12,32,33] which provides the expansion of t_{MF} only up to linear order in q and which is adequate only for inhomogeneous potentials with sufficiently large η . Note that these papers express the result for $D_1(\eta)$ in terms of an equivalent sum representation which, however, is less convenient numerically.

In Eq. (31) for $D_1(\eta)$, the integrand essentially contains the leading-order density modifications that are induced by the atomic interactions — they are described by the given combination of Bose functions — weighted with the equipotential surface area of Eq. (6). The integration extends over the whole configuration space available to the Bose gas. The term $D_1(\eta)q$ thus expresses the large-scale influence of the potential shape and the density modifications on the transition temperature. The term $D'(\eta)q^{2\eta}$ is of a very different origin. It is determined by the behavior of $f_{cr}^{MF}(x)$ within the small region $0 \leq x \lesssim q^2$ near the trap center. In the expression for $D_2(\eta)$, the integral is to be understood as regularized with respect to the divergence at $x=0$ which arises for $\eta < 1$ [40]. The term quadratic in q is most important around $\eta=1$ where it counterbalances the divergence of the term $D'(\eta)q^{2\eta}$. It is of minor significance, however, regarding the qualitative aspects of the behavior of t_{MF} . In the following discussion, we thus focus on the first two terms in the expansion (30).

B. Renormalization-group theory

In renormalization-group theory, the degeneracy function of a homogeneous Bose gas with thermodynamic parameters $M(0)$, $\tilde{G}(0)$, and $b(0)$ is given by

$$\begin{aligned}
 f^{RG}(M(0), \tilde{G}(0), b(0)) &\equiv n_{hom}^{RG} \lambda_T^3 \\
 &= - \sqrt{\frac{2}{\pi}} b^{3/2}(0) \frac{\partial}{\partial M(0)} \\
 &\quad \times I(M(0), \tilde{G}(0), b(0); \eta = 1/2).
 \end{aligned} \tag{34}$$

Given a critical trajectory with initial conditions $(M_{cr}(0), \tilde{G}_{cr}(0), b_{cr}(0))$, we obtain from Eq. (34) the critical degeneracy pertaining to the corresponding value of $q = a/\lambda_T = \tilde{G}_{cr}(0)b_{cr}(0)/[4\pi + 2\tilde{G}_{cr}(0)b_{cr}(0)/\pi]$ [cf. Eq. (25)]. The critical degeneracy function is thus given by

$$f_{cr}^{RG}(x) = f^{RG}(M_{cr}(0) - x/b_{cr}(0), \tilde{G}_{cr}(0), b_{cr}(0)). \tag{35}$$

This expression follows from the relation $\beta_\Lambda[\mu - V(\mathbf{x})] = M(0) - x/b_{cr}(0)$. Note that all flow trajectories used for the evaluation of f_{cr}^{RG} have the same interaction parameter $q = a/\lambda_T$. The comparison between the RG-LDA and the RG theory of Sec. III provides an important consistency check for our methods. If they are to be reliable, the results should not be too different.

In Ref. [13] a variant of the mean-field approach of Sec. IV A was proposed that allows us to include in a simple way the influence of critical fluctuations on the condensation temperature in the trap. It is based on the assumption that the main effect of these fluctuations is to lower the critical degeneracy $f_{cr}(0)$, at which condensation sets in at the trap center. The further behavior of $f_{cr}(x)$, however, is still modeled with the help of the mean-field LDA expressions (26) and (28) with a suitably chosen critical μ . The main difficulty in the implementation of this approach consists of course in determining the modified critical degeneracy. We choose the value obtained from the RG description of the homogeneous interacting gas at a given $q = a/\lambda_T$. As this is also the critical degeneracy used in the RG-LDA, the comparison between the two methods allows us to assess how sensitive the results are with regard to the different approximations to the behavior of the function $f_{cr}(x)$.

V. NUMERICAL RESULTS

In this section, we discuss numerical results for the critical temperature T_c determined according to the different methods outlined in Secs. III and IV. As to the RG calculations, we focus on the ε expansion for the reasons indicated in Sec. III, but we comment on respective results obtained from the flow equations (20) whenever appropriate.

Figure 1 shows the shift in the critical temperature $t = T_c/T_c^0 - 1$ (relative to the critical temperature T_c^0 of an ideal gas with the same particle number) as a function of the potential shape parameter η for fixed values of $q = a/\lambda_T$. We compare results from the ε expansion (bold curves) to the mean-field LDA (dashed). The value of $q = 10^{-2}$ in Fig. 1(b) is in the regime of current experiments [20], whereas $q = 10^{-5}$ [Fig. 1(a)] is more of interest for theoretical studies.

First of all, we observe that the RG results reproduce very well the qualitative behavior of the critical temperature pre-

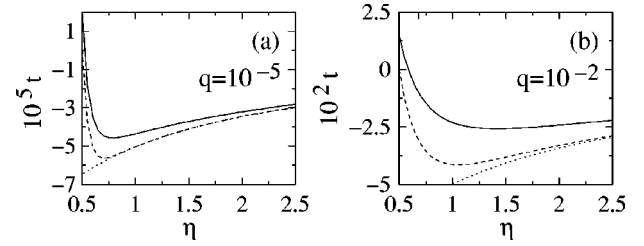


FIG. 1. Relative shift t of critical temperature as a function of η at fixed $q = a/\lambda_T = 10^{-5}$ (a) and 10^{-2} (b). Bold curves: RG results with ε expansion. Dashed curves: mean-field LDA. Dotted curves: linear mean-field approximation $D_1(\eta)q$ [cf. Eqs. (30) and (31)].

dicted by mean-field theory—for example, the minimum in the $t(\eta)$ graphs. As MFT can be trusted as a first approximation, this observation clearly indicates the general validity of our RG approach. In particular, it shows that the agreement for the harmonic oscillator found previously [11] was not merely a coincidence. We also see that the RG results always predict a higher critical temperature than MFT. Such an increase was previously reported in studies of the harmonic oscillator [10,13,15] and can be attributed to the remaining influence of critical long-wavelength fluctuations. It should also be mentioned that — as discussed in Ref. [11] — the RG results for the homogeneous case ($\eta=0.5$) agree well with the most accurate calculations currently available [5,6].

For large η and small q , the MFT approach is supposed to become more and more accurate as the effect of critical fluctuations is diminished. In fact, our RG results approach MFT in this limit. However, at $\eta=2$, for example, which corresponds to the harmonic oscillator potential, there is still a small difference in the shifts (about 7%) which seems to persist even in the limit of $q \rightarrow 0$. This difference might indicate that the RG slightly overestimates the influence of critical fluctuations [11]; on the other hand, the accuracy of the MFT is not known precisely, as well.

For the parameter values shown in Fig. 1, the difference between the RG results with and without ε expansion is always much smaller than the distance to the MFT values. Differences between the RG calculations become more pronounced as q grows; at fixed q , they are largest around $\eta = 0.5$ and then decrease rapidly.

A further interesting aspect of Fig. 1 concerns the fact that one can distinguish between different regimes in the behavior of T_c as the potential shape parameter η is varied. The region of large η can be characterized as “inhomogeneous.” There, the shift in T_c is well described by the first term $D_1(\eta)q$ of the mean-field expression (30) (compare with the dotted curves in Fig. 1). As explained in Sec. IV A, the shift is thus essentially determined by the global shape of the external trapping potential and the large-scale atomic density distribution in the presence of the interactions. Effects beyond first-order mean-field theory, such as critical fluctuations, only play a minor role as long as q is not too large. The inhomogeneous regime begins after the minimum in the $t(\eta)$ curves, approximately.

In the region to the left of and around the minimum, physical effects at low energies near the potential minimum play an essential role in the behavior of the critical tempera-

ture. Partially, these effects can still be described within mean-field theory—i.e., by the term $D'(\eta)q^{2\eta}$ of Eq. (30), which together with $D_1(\eta)q$ provides an excellent approximation to the exact mean-field result for small values of q , such as in Fig. 1(a) [40]. The term $D'(\eta)q^{2\eta}$ on its own gives rise to the increase in the mean-field shift $t(\eta)$, as η approaches 0.5 from the right [compare the dashed and dotted curves in Fig. 1(a)]. As stated at the end of Sec. IV A, the term reflects the behavior of the critical degeneracy $f_{(cr)}^{MF}$ at small x —i.e., for low energies near the trap center. On the other hand, as it is apparent from Fig. 1, in the “low-energy regime,” effects beyond mean-field theory are also much more prominent. These effects are included in the RG theory. They are mainly due to critical fluctuations which occur near the trap center where the actual phase transition sets in.

For growing interaction strength q , the crossover between the two different regimes becomes less pronounced. On the one hand, the significance of effects beyond mean field is increased in general; on the other hand, in the mean-field expression (30) higher-order terms become important which are less straightforward to interpret.

In experiments with ultracold atomic Bose gases, only the mean-field shift of the critical temperature has been identified unambiguously so far [20]. In harmonic traps (i.e., $\eta = 2$), which were used in these experiments, effects beyond MFT are small and therefore hard to detect. For further experimental studies in this direction, it would be desirable to optimize the trapping potentials to make the effects in question most pronounced. Our results provide some guidance in this direction as they show that anharmonic traps with η less than 2 might be suitable for this purpose. First of all, we note from Eq. (9) that, at fixed particle number and trap size V_{char} , the condensation temperature rises with decreasing η . Let us now consider the case of Fig. 1(b) with $q=10^{-2}$, which is a typical experimental value. If one trusted MFT, a trap with η around 1 would be favorable, as there the MFT shift in T_c is largest. However, MFT may no longer be applicable for such traps. In order to detect the influence of critical fluctuations, traps with η around 0.75 should be used as there the difference between RG theory and MFT is found to be maximum and about 2.4 times the amount at $\eta=2$. Finally, RG theory alone predicts the shift in T_c to be biggest around $\eta=1.5$; however, the difference to $\eta=2$ is not very large.

It should not be too difficult in practice to engineer traps with η less than 2. A trap which is harmonic in one or two spatial dimensions and quasihomogeneous in the remaining one(s) would have $\eta \approx 1$ or 1.5, respectively. Such traps can be manufactured with current technology.

Figure 2 depicts the relative shift t in the critical temperature as a function of a/λ_T^0 for various values of η (note the scaling of a with λ_T^0 , the thermal wavelength pertaining to the ideal gas). These results were obtained with the ε expansion of Sec. III. In the figure, the calculations are extended up to large values of a/λ_T^0 . It turns out that for a/λ_T^0 exceeding, approximately, 0.1, the numerical results for t become dependent on the cutoff Λ used in the integration of the flow equations. In Ref. [11], we have discussed this cutoff dependence. It was shown that our RG model can be interpreted as describing a gas of hard-sphere bosons with a finite-height

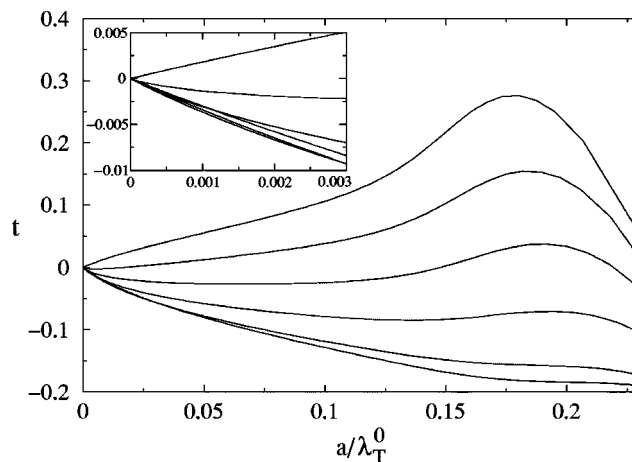


FIG. 2. Relative shift t of the critical temperature as a function of a/λ_T^0 for $\eta=0.5, 0.6, 0.75, 1.0, 1.5$, and 2.0 (from top to bottom). Shown is the RG calculation with ε expansion.

repulsive interaction potential. If the interaction parameter a/λ_T^0 becomes large enough, the critical temperature no longer depends only on the scattering length a , but is also sensitive to finer details of the interaction. A change in the cutoff, for example, corresponds to a variation of the hard-sphere radius. In spite of the cutoff dependence of the quantitative results, the qualitative behavior of the curves is not affected, so that we focus here on these qualitative aspects.

In particular, we wish to point out two aspects of Fig. 2 that might be relevant to experimental studies. Recently, much effort has been invested in calculations of T_c for small scattering lengths in the homogeneous Bose gas, a problem which is of significant theoretical relevance [4]. From the inset in Fig. 2 (as well as from Fig. 1), we can see that, for small a/λ_T^0 , the critical temperature is very sensitive to deviations from an exactly homogeneous trapping potential (note that here the cutoff dependence of the RG results is not an issue). For example, going from $\eta=0.5$ to 0.6 (which corresponds to an r^{30} potential) leads to a drop in T_c instead of an increase. For accurate experimental measurements of the critical temperature of homogeneous Bose gases, this sensitivity on the trapping potential might thus be a serious obstacle in the range of small a/λ_T^0 .

On the other hand, if we focus on the qualitative behavior at large scattering lengths, we observe features that are much less susceptible to variations of the potential shape. In particular, for η up to about 1.0, the critical temperature as a function of a/λ_T^0 displays a pronounced maximum whose position changes only little with η . We note that the position and height of the maximum agree qualitatively with the theoretical results of [41]. Furthermore, in the experiment [42], that studied the phase transition in the ^4He -Vycor system, a maximum in the condensation temperature was found at a value of a/λ_T^0 that is consistent with Fig. 2. The present results indicate that the location of this maximum might in fact not be too sensitive on the details of the external potential. We find the height of the maximum to depend more strongly on the potential, however, and it should be noted that the value measured in [42] is much larger than the theoretical results.

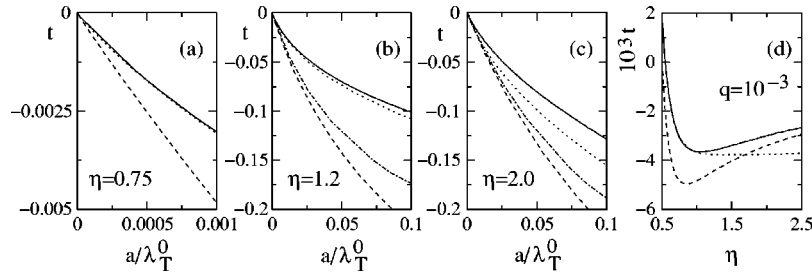


FIG. 3. Comparison between the RG method of Sec. III and RG-LDA. (a)–(c) display the relative shift t of the critical temperature as a function of a/λ_T^0 for $\eta=0.75$ (a), $\eta=1.2$ (b), and $\eta=2.0$ (c). (d) shows $t(\eta)$ for $q=10^{-3}$. Bold curves: RG method of Sec. III. Dotted curves: RG-LDA. Dashed curves: MFT. Dot-dashed curves: modified MFT according to [13]. All RG calculations use the ε expansion.

Finally, we remark that there is a qualitative difference between the RG results with and without ε expansion, which appears at larger values of η and a/λ_T^0 . For $\eta=2.0$, for example, the RG result without ε expansion keeps increasing almost linearly after a certain value of a/λ_T^0 . Besides the arguments mentioned in Sec. III, this behavior, which is probably unphysical, provides another reason that leads us to prefer the ε expansion [11].

In Fig. 3, we compare the RG approach of Sec. III to the RG local-density approximation described in Sec. IV B. All RG calculations make use of the ε expansion. Figures 3(a)–3(c) show the relative shift t in the critical temperature as a function of a/λ_T^0 for various values of η , whereas (d) depicts $t(\eta)$ for $q=a/\lambda_T=10^{-3}$. From these results we conclude that the two RG methods agree very well for values of η up to about 1.25. Figures 3(a) and 3(b) are drawn for different ranges of values for a/λ_T^0 in order to emphasize that this agreement holds on all scales of a/λ_T^0 up to 0.1.

Going to larger values of η , however, we find that the two methods soon start to deviate appreciably from each other [Figs. 3(c) and 3(d)]. The reason for these discrepancies is due to some deficiencies of the ε expansion. As noted in Sec. III, the ε expansion is expected to be valid in the vicinity of the phase transition. When applying the LDA at increasingly large η , however, the behavior of the degeneracy function f_{cr}^{RG} at values of x far away from the phase transition becomes more and more relevant [cf. Eq. (27)]. In this region of large x , the ε expansion ceases to be applicable. An indication of this failure is the fact that, for $x \rightarrow \infty$, f_{cr}^{RG} does not converge towards the correct asymptotic form: i.e., the degeneracy function of the ideal gas. In fact, if we artificially modify f_{cr}^{RG} to behave correctly at large x , the agreement of the RG-LDA method with the RG approach is considerably improved.

From these results we conclude that the RG method of Sec. III is consistent with the RG-LDA, as long as the latter requires the degeneracy function only in the vicinity of the phase transition. This restriction on the applicability of the RG-LDA has to be expected from the nature of the ε expansion. Nevertheless, the very good agreement at small η provides further evidence for the reliability of the RG approach of Sec. III. We note that although this method also applies the ε expansion, it only makes use of the properties of critical trajectories, so we expect it to be accurate for larger η as well.

In this context, it is instructive to compare the RG-LDA results with the modified mean-field method of Ref. [13] that

was discussed at the end of Sec. IV B. In our context, this method amounts to using a degeneracy function that coincides with f_{cr}^{RG} at $x=0$, but whose further behavior is calculated from MFT. We see from Figs. 3(b) and 3(c) that this approach strongly deviates from the RG-LDA results even at small η (a similar behavior was also found at $\eta=0.75$). This shows that the local-density calculations sensitively depend on the details of the degeneracy function and that an agreement between the RG-LDA and RG methods cannot be expected *a priori*.

Finally, it should be mentioned that without the ε expansion, f_{cr}^{RG} indeed assumes the correct asymptotic form for $x \rightarrow \infty$. In this case, the RG-LDA agrees better with the RG method at larger values of η ; at small η , however, the behavior is not as well reproduced as with the ε expansion.

VI. SUMMARY AND CONCLUSIONS

In this paper, we have investigated the phase transition of interacting Bose gases in general power-law traps in the thermodynamic limit. To this end, we have compared various theoretical approaches. Our main focus was on evaluating the partition function above the transition point with the help of the renormalization group. Applying a modification of Wilson's momentum-shell renormalization and the ε expansion, we derived flow equations for the chemical potential and the interaction constant that do not depend on the specific trapping potential. The properties of the trap enter only into the flow equation for the free energy. Our RG approach allows a unified description of homogeneous and quasihomogeneous as well as strongly inhomogeneous Bose gases.

The RG approach was applied to calculate the transition temperature of the trapped interacting Bose gas. We compared the RG results to mean-field theory as well as to a local-density approximation based on the RG description of the homogeneous Bose gas. MFT is expected to be quantitatively reliable only for sufficiently inhomogeneous potentials—e.g., harmonic traps—but it yields a useful first approximation also for quasihomogeneous systems. MFT and RG results were found to be in good qualitative agreement. The comparison between MFT and RG allowed us to assess the influence of long-wavelength critical fluctuations on the transition temperature and their dependence on the trapping potential. The nonperturbative critical fluctuations are properly accounted for in the RG theory, but neglected in MFT. Furthermore, we were able to identify different re-

gimes in the behavior of the critical temperature as the potential shape is varied. We distinguished a regime near the homogeneous limit, where effects at low energies near the potential minimum are essential, and an inhomogeneous regime, where the transition temperature is determined by the overall behavior of the external trapping potential. Based on the analysis of our results for T_c , we also made some suggestions for optimizing the trap design in experiments that study the transition temperature.

The RG-based local-density approximation was found to agree well with our main RG method provided the potentials are not too inhomogeneous. These results show the self-consistency of the RG approach and provide further evidence for the reliability of the method presented. Deviations of the RG-LDA for more strongly inhomogeneous potentials could

be traced back to the fact that in these cases the ε expansion is no longer applicable.

Finally, we want to point out that all our results equally apply to isotropic as well as anisotropic potentials. In the thermodynamic limit they are all essentially characterized by the shape parameter η .

ACKNOWLEDGMENTS

This work was supported by the Deutsche Forschungsgemeinschaft through the Forschergruppe ‘‘Quantengase.’’ G.M. wishes to thank I. J. R. Aitchison for many valuable discussions. We also gratefully acknowledge stimulating discussions with H. Kleinert and A. Pelster.

-
- [1] M. H. Anderson, J. R. Ensher, M. R. Matthews, C. Wieman, and E. A. Cornell, *Science* **269**, 198 (1995).
 - [2] K. B. Davis, M. O. Mewes, M. R. Andrews, N. J. van Druten, D. S. Durfee, D. M. Kurn, and W. Ketterle, *Phys. Rev. Lett.* **75**, 3969 (1995).
 - [3] C. C. Bradley, C. A. Sackett, J. J. Tollett, and R. G. Hulet, *Phys. Rev. Lett.* **75**, 1687 (1995).
 - [4] See, e.g., J. O. Andersen, *Rev. Mod. Phys.* (to be published), e-print cond-mat/0305138, and references therein.
 - [5] V. A. Kashurnikov, N. V. Prokof'ev, and B. V. Svistunov, *Phys. Rev. Lett.* **87**, 120402 (2001).
 - [6] P. Arnold and G. D. Moore, *Phys. Rev. E* **64**, 066113 (2001).
 - [7] S. Giorgini, L. P. Pitaevskii, and S. Stringari, *Phys. Rev. A* **54**, R4633 (1996).
 - [8] H. J. Davies and C. S. Adams, *Phys. Rev. A* **55**, R2527 (1997).
 - [9] J. Tempere, F. Brosens, L. F. Lemmens, and J. T. Devreese, *Phys. Rev. A* **61**, 043605 (2000).
 - [10] T. Bergeman, D. L. Feder, N. L. Balazs, and B. I. Schneider, *Phys. Rev. A* **61**, 063605 (2000).
 - [11] G. Metikas, O. Zobay, and G. Alber, *Phys. Rev. A* **69**, 043614 (2004).
 - [12] H. Shi and W.-M. Zheng, *Phys. Rev. A* **56**, 1046 (1997).
 - [13] M. Houbiers, H. T. C. Stoof, and E. A. Cornell, *Phys. Rev. A* **56**, 2041 (1997).
 - [14] S. K. Adhikari and A. Gammal, *Physica A* **286**, 299 (2000).
 - [15] P. Arnold and B. Tomásik, *Phys. Rev. A* **64**, 053609 (2001).
 - [16] S. Liu, G. Huang, L. Ma, S. Zhu, and H. Xiong, *J. Phys. B* **33**, 3911 (2000).
 - [17] H. Xiong, S. Liu, G. Huang, Z. Xu, and C. Zhang, *J. Phys. B* **34**, 3013 (2001).
 - [18] H. Suzuki and M. Suzuki, *Int. J. Mod. Phys. B* **15**, 2335 (2001).
 - [19] S. Pearson, T. Pang, and C. Chen, *Phys. Rev. A* **58**, 4796 (1998).
 - [20] F. Gerbier, J. H. Thywissen, S. Richard, M. Hugbart, P. Bouyer, and A. Aspect, *Phys. Rev. Lett.* **92**, 030405 (2004).
 - [21] M. Bijlsma and H. T. C. Stoof, *Phys. Rev. A* **54**, 5085 (1996).
 - [22] G. Alber, *Phys. Rev. A* **63**, 023613 (2001).
 - [23] V. Bagnato, D. E. Pritchard, and D. Kleppner, *Phys. Rev. A* **35**, 4354 (1987).
 - [24] M. Li, L. Chen, and C. Chen, *Phys. Rev. A* **59**, 3109 (1999).
 - [25] Z. Yan, M. Li, L. Chen, C. Chen, and J. Chen, *J. Phys. A* **32**, 4069 (1999).
 - [26] Z. Yan, *Phys. Rev. A* **61**, 063607 (2000).
 - [27] L. Salasnich, *J. Math. Phys.* **41**, 8016 (2000).
 - [28] O. Mulken, P. Borrmann, J. Harting, and H. Stamerjohanns, *Phys. Rev. A* **64**, 013611 (2001).
 - [29] H. Shi and W.-M. Zheng, *Phys. Rev. A* **56**, 2984 (1997).
 - [30] S. Pearson, T. Pang, and C. Chen, *Phys. Rev. A* **58**, 4796 (1998).
 - [31] M. Bayindir, B. Tanatar, and Z. Gedik, *Phys. Rev. A* **59**, 1468 (1999).
 - [32] L. Salasnich, *Int. J. Mod. Phys. B* **16**, 2185 (2002).
 - [33] H. Suzuki and M. Suzuki, *Int. J. Mod. Phys. B* **17**, 2439 (2003).
 - [34] K. G. Wilson and J. Kogut, *Phys. Rep.*, *Phys. Lett.* **12C**, 75 (1974).
 - [35] R. J. Creswick and F. W. Wiegel, *Phys. Rev. A* **28**, 1579 (1983).
 - [36] G. Metikas and G. Alber, *J. Phys. B* **35**, 4223 (2002).
 - [37] L. D. Landau and E. M. Lifshitz, *Quantum Mechanics: Non-Relativistic Theory* (Pergamon, Oxford, 1977).
 - [38] G. Metikas, O. Zobay, and G. Alber, *J. Phys. B* **36**, 4595 (2003).
 - [39] L. P. Pitaevskii and S. Stringari, *Bose-Einstein Condensation* (Oxford University Press, Oxford, 2003).
 - [40] O. Zobay, *J. Phys. B* **37**, 2593 (2004).
 - [41] P. Grüter, D. Ceperley, and F. Laloë, *Phys. Rev. Lett.* **79**, 3549 (1997).
 - [42] J. D. Reppy, B. C. Crooker, B. Hebral, A. D. Corwin, J. He, and G. M. Zassenhaus, *Phys. Rev. Lett.* **84**, 2060 (2000).